

# A Mathematical Model for The Performance of Solar Heating Driven Bubble Pumps

Khaled Elshawesh<sup>1\*</sup>, Khairy Agha<sup>2</sup>, and Elhadi Dekam<sup>2</sup>

<sup>1\*</sup> M.Sc. Senior Engineer; The Central Board for Research and Manufacture, Tripoli, Libya;

<sup>2,3</sup> Professor in Mechanical and Industrial Engineering Department, Faculty of Engineering, University of Tripoli, Tripoli, Libya.

e-mail: <sup>1</sup> [kelshawesh@yahoo.com](mailto:kelshawesh@yahoo.com), <sup>2</sup> [k\\_r\\_gha@yahoo.com](mailto:k_r_gha@yahoo.com) <sup>3</sup> [e.dekam@uot.edu.ly](mailto:e.dekam@uot.edu.ly)

**Abstract:** A mathematical model of the bubble pump is established by employing the governing equations; the continuity, momentum and energy equations. The model was used to evaluate the performance of the pump under different geometrical and operational conditions. Different parameters including the pump tube diameter, the pumping head, and solar heating input were considered in the analysis. The flow rates of both phases (liquid and vapor) were predicted for each set of parameters. Methanol was used as the working fluid. The performance is presented for a number of different scenarios. The flow was found to be increased with both larger diameters and low static heads, while it has a roughly sine curve with the heat input. A set of results show that for a tube diameter of 10 mm and pumping head of 450 mm, increasing the heat input from 300 W to 500 W increases the mass flow rate of vapor from 0.04 kg/sec to 0.08 kg/sec, while the liquid flow increases from 0.075 kg/sec to 0.22 kg/sec, respectively. Generally, the results of this study were found to be in fair agreement with published results.

## نموذج رياضي لدراسة الأداء لمضخة فقاعية تعمل بالطاقة الشمسية الحرارية

خالد الشواشي<sup>1</sup>، خيري اغا<sup>2</sup> والهادي الدكام<sup>3</sup>

اللجنة المركزية للبحوث والصناعة. طرابلس-ليبيا

<sup>3</sup> قسم الهندسة الميكانيكية-كلية الهندسة. جامعة طرابلس-ليبيا

ملخص: تم بناء نموذج رياضي للمضخة الفقاعية باستخدام المعادلات الحاكمة، معادلات الاستمرارية والزخم والطاقة. وقد استخدم النموذج في تقييم أداء المضخة تحت ظروف هندسية وتشغيلية مختلفة. وقد تم الأخذ في الاعتبار عوامل مختلفة بما في ذلك قطر أنبوب المضخة، عمود الضخ، ومقدار الطاقة الشمسية، في التحليل. تم توقع معدلات التدفق للطورين (سائل وبخار) لكل سلة من العوامل.

\* Corresponding author

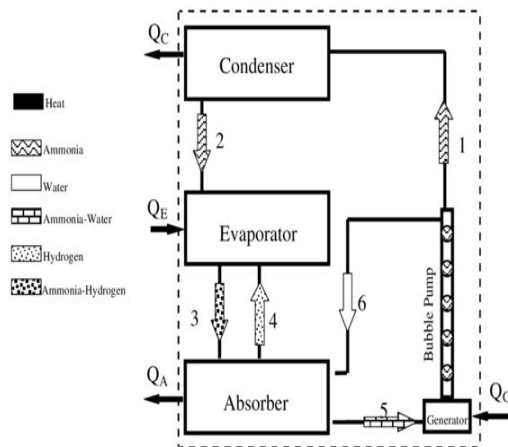
استخدم الميثانول كسائل تشغيل. وتم تقديم الأداء لعدد من السيناريوهات المختلفة. وقد وجد أن التدفق يزداد مع الأقطار الأكبر عمود رفع منخفض، في حين أن لها تقريباً شكل منحني الجيب مع الحرارة الداخلة. وتظهر مجموعة من النتائج أن عند استخدام أنبوب بقطر 10 مم وعمود ضخ 450 مم، زاد الحرارة الداخلة من 300 واط إلى 500 واط وازداد معدل التدفق الكلي للبخار من 0.04 كجم/ثانية إلى 0.08 كجم/ثانية، بينما ازداد تدفق السائل من 0.075 كجم/ثانية إلى 0.22 كجم/ثانية، على التوالي. وبوجه عام، تبين أن نتائج هذه الدراسة في انضاق مقبول مع النتائج المنشورة.

**Keywords:** Bubble pump, two phase flow, lifting liquids with thermal heating.

## 1. INTRODUCTION

Both photovoltaic and solar thermal energy systems have been used over the last few decades to cover the refrigeration needs for both domestic and industrial purposes. Ullah et al. [1] presented a review covers different solar thermal refrigeration systems, with an attention to solar absorption refrigeration and solar adsorption refrigeration systems employing various working fluids.

The main components of vapor absorption refrigeration systems are the absorber, generator, condenser, and evaporator, as indicated in Figure (1). A pump is a critical component of the system for circulating the refrigerant-absorbent solution from the low pressure absorber to the high pressure generator. A thermally-driven bubble pump can be powered by solar thermal energy. In such cycles, a bubble pump can be used to lift the solution from the absorber to the generator while it desorbs the refrigerant vapor. Theoretical and experimental work has been conducted in order to test the bubble pump for vapor absorption refrigeration systems. The pump model was validated with water at atmospheric conditions. The bubble pump tube diameters are taken as 6 to 10 mm and at different heat inputs [2].



Q=Heat, 1 & 2=Ammonia, 3=ammonia-Hydrogen, 4=Hydrogen, 5=Ammonia-Water, 6=Water

Figure (1). A Diffusion-Absorption Cycle.

A bubble pump is a fluid pump that uses solar thermal energy to lift liquid from a lower level reservoir to a higher level reservoir. It does not contain any moving parts [3]. The bubble pump, as shown in Figures 2, is nothing but a vertical tube of relatively small circular cross-section attached to upstream and downstream reservoirs [4]. The idea of this heat driven bubble pump has been first applied in single pressure absorption

refrigeration systems, such as the Platen and Munters diffusion-absorption cycle and Einstein cycle in 1928.

Delano [3] addressed the design of a bubble pump for use in a single pressure absorption refrigeration cycle by utilizing the principle of momentum balance and carefully treated the slip condition between the phase velocities of the two-phase flow. Sathe [5] used Delano's model and evaluated the performance of the bubble pump both analytically and experimentally, and his results were used to derive a relationship between heat input and mass flow rate of vapor, mass flow rate of liquid, and pumping ratio. Susan Jennifer [6] worked on bubble pump design and performance. She carried out experimental studies and her results were compared with previous models. Recently, a research paper authored by Koyfman, et al [7], where it studied the performance of the bubble pump for diffusion refrigeration units and concluded that a low driving head is recommended to achieve higher flow rates.

Benhmidene et al. [8] provide a literature review on bubble pump used in diffusion-absorption refrigeration systems. A numbers of bubble pump configurations are considered. Han-Shik et al. [9] developed a new solar water heater system using a solar bubble pump instead of an electric pump. An evacuated tube collector is employed to generate steam that used to operate the pump. The proposed system is compared with the conventional solar water heaters. They show that the bubble system achieves an efficiency of 10% higher than that of the conventional electric pump system.

In a solar driving bubble pump, the solar collector acts as the generator. Evacuated tube collectors are considered to have high efficiency, medium price, and commercial availability. A single and multiple lift tube indirectly or directly solar heated bubble pump are used [10]. The performance of three different indirectly heated, solar powered bubble pumps/generators were investigated and discussed [11]. The disadvantage of these systems is a very low COP. Therefore, the configuration of the generator and bubble pump is of great importance. In order to increase the COP, it must utilize minimum heat as possible and desorb as much refrigerant as possible from the solution [10].

The equation of Chilshom and Taitel is used by Jakob et al. [12] to dimension the tube diameter pump, where slug flow was calculated for tubes with an inner diameter ranging from 5 to 41 mm. To study the boiling flow stability in the solar bubble pump, Benhmidene et al. [13] used a drift model. The pressure drop in the bubble pump was predicted. The result shows the influence of heat flux input in the bubble pump and the mass flux on the stability of flow in the pump.

In the present study, a mathematical model of the bubble pump was developed by using derived equations based on the continuity momentum and energy equations. Under different geometrical and operating conditions, this model is employed to evaluate and assess the bubble pump characteristics, including the determination of the flow rates of the pumped liquid and vapor. In order to validate and evaluate the achieved mathematical model, the obtained results are compared with theoretical and experimental results of recently published research studies.

## **2. MATHEMATICAL MODEL**

The basic governing equations; the continuity, momentum, and energy conservation equations were used to develop the required mathematical model [14]. Bernoulli's equation is employed to derive the submergence ratio,  $h/L$ , which describes the average pressure gradient along the lift tube. The model is divided into two partial flow fields as indicated below; liquid phase flow region along the unheated tube and two phase flow region along the driven vertical heated column. The model developed with the objective of obtaining results that can be instructive in demonstrating how the heat driven bubble pump, depicted in Figure 2, operates in practice. Here, the heat transfer takes place along the vertical tube as indicated in the Figure.

### A. Liquid Phase Flow

The liquid phase flow, assigned by the letter “f”, was predicted by evaluating the liquid flow out of the lower reservoir to the entry of the bubble pump vertical heated tube, as indicated in Figure 2. Here, the flow is considered to be an incompressible flow with negligible pressure loss. Bernoulli’s equation can be applied along a streamline connecting the liquid free surface of the lower reservoir with the entry section of the tube at point 1 in Figure 2. Then the static pressure at the entrance of the pipe can be written as:

$$P_1 = P_0 + \rho_f gh - \frac{1}{2} \rho_f V_1^2 \quad (1)$$

Where  $P_0$  is the ambient static pressure at the free surface of the lower reservoir,  $\rho_f$  is the density of the liquid,  $h$  is the static head difference,  $g$  is the acceleration of gravity, and  $V_1$  is the tube fluid velocity at point 1.

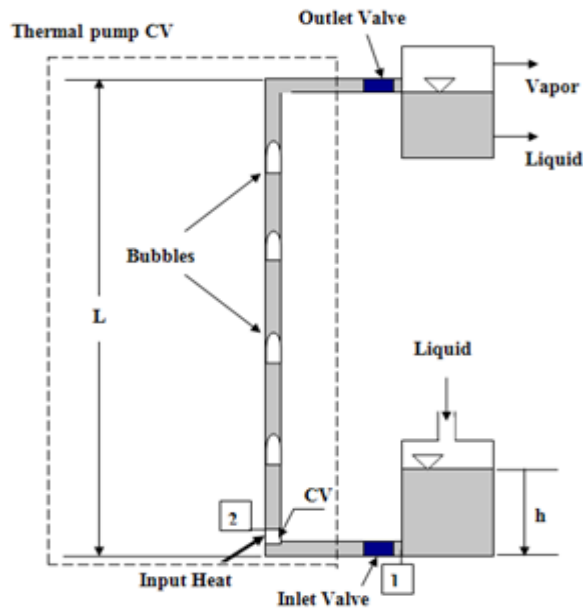


Figure (2). Thermal Bubble Pump Control Volume.

A small control volume is taken at the beginning of the lift tube, as shown in Figure 2. As this control volume positioned at the start of the heated column, it is assumed that the only liquid phase enters this control volume, while a mixture of vapor bubbles and liquid leave this control volume. The continuity equation applies to the indicated heated control volume, hence, the mixture velocity at the exit of the control volume,  $V_2$ , can be written as [15];

$$V_2 = V_1 \left( 1 + \frac{\dot{V}_g}{\dot{V}_f} \right) \quad (2)$$

Where  $\dot{V}_g$  is the volumetric flow rate of the vapor and  $\dot{V}_f$  is the volumetric flow rate of the liquid.

### B. Liquid Momentum Equation

The equation of momentum applies to the indicated control volume, while the frictional effects on the control surface are very small and can be neglected. Therefore, the static pressure at the outlet section can be determined by the following relationship;

$$P_2 = P_1 + \rho_f V_1 (V_2 - V_1) \tag{3}$$

Where, P is the static pressure, and V is the flow velocity. Employing equations (1) and (2), we may have;

$$P_2 = P_0 + \rho_f gh - \frac{1}{2} \rho_f V_1^2 + \frac{\rho_f V_1 \dot{V}_g}{A} \tag{4}$$

Where A is the cross-sectional area of the lift tube.

### C. Two Phase Flow

The flow along the heated column, which extends from point 2 to the end of the vertical tube, is classified as two phase flow consisting of vapor bubbles and liquid of the working solution. The governing equations would be applied to the control volume in this region.

#### i. Two Phase Continuity Equation

Conservation of mass is applied along the lift tube starting from point 2. In addition to that, a number of relationships, related to the two phase flow behavior, were used for the sake of simplification and for use in the forthcoming equations in the appropriate manner. These can be written and interpreted in the following arrangements; the mass of the vapor is coming from the same mass of the liquid, hence;

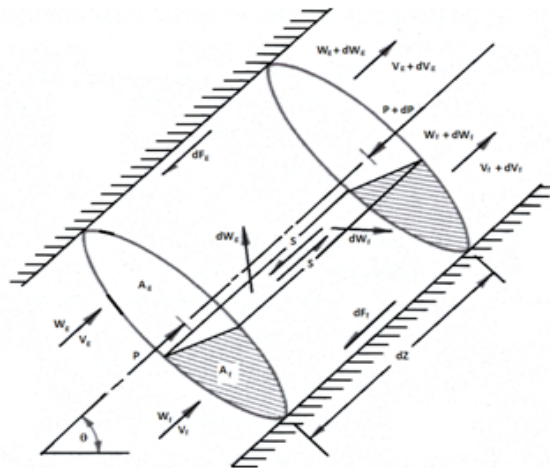


Figure (3). A simplified model for two-phase over an element of lift tube.

$$d\dot{m}_g = - d\dot{m}_l \tag{5}$$

The vertical gas mass flow rate gradient is;

$$\frac{d\dot{m}_g}{dz} = \frac{d}{dz} (A_g \rho_g V_g) \tag{6}$$

The vertical liquid mass flow rate gradient is;

$$\frac{d\dot{m}_f}{dz} = \frac{d}{dz}(A_f \rho_f V_f) \quad (7)$$

## ii. Two Phase Momentum Equation

Referring to the control volume, Figure (3), the momentum equation can be applied for vapor and liquid phases, separately. As well known, the summation of all acting forces on the control volume should equal to the rate of change of momentum. Thus, for the vapor phase, the equation is;

$$-A_g dP - dF_g - S - A_g dz \rho_g g = \dot{m}_g dV_g + V_g d\dot{m}_g - V_f d\dot{m}_g \quad (8)$$

While for the liquid phase, the equation takes the form;

$$-A_f dP - dF_f + S - A_f dz \rho_f g = \dot{m}_f dV \quad (9)$$

Adding Eq. (8) to Eq. (9) and using Eq. (5), results in

$$-AdP - dF_g - dF_f - g dz (A_f \rho_f + A_g \rho_g) = d(\dot{m}_g V_g + \dot{m}_f V_f) \quad (10)$$

The net frictional force acting on each phase may be expressed in terms of the areas occupied by each phase. Thus;

$$\begin{aligned} (dF_g + S) &= -A_g \left( \frac{dP}{dz} \right)_{gF} dz \\ (dF_f - S) &= -A_f \left( \frac{dP}{dz} \right)_{fF} dz \\ (dF_g + dF_f) &= -A \left( \frac{dP}{dz} \right)_F dz \end{aligned} \quad (11)$$

Where F is the frictional force, S is the force due to the gas-liquid interface,  $A_g$  is the cross-sectional area occupied by gas, and  $(dp/dz)_{gF}$  is the pressure gradient due to the frictional force in gas phase. Substitution of Eq. (11) into Eq. (10), gives;

$$-AdP - \left( -A \left( \frac{dP}{dz} \right)_F dz \right) - g dz (A_f \rho_f + A_g \rho_g) = d(\dot{m}_g V_g + \dot{m}_f V_f) \quad (12)$$

Divide equation (12) by the element volume  $Adz$ , one can find the pressure gradient along pump tube as follows;

$$\frac{dP}{dz} = \left( \frac{dP}{dz} \right)_F + \left( \frac{dP}{dz} \right)_z + \left( \frac{dP}{dz} \right)_a \quad (13)$$

Where  $(dp/dz)_F$  is the pressure gradient due to friction,  $(dp/dz)_z$  is due to the static head, and  $(dp/dz)_a$  is due to the fluid acceleration. Now, expand each term as follows;

$$-\left( \frac{dP}{dz} \right)_F = \frac{1}{A} \frac{d}{dz} (F_g + F_f) = \frac{1}{A} \frac{dF}{dz} \quad (14)$$

By using the known relationships for the two-phase flow, the other two terms are;

$$-\left( \frac{dP}{dz} \right)_z = g(\alpha \rho_g + (1 - \alpha) \rho_f) \quad (15)$$

$$-\left( \frac{dP}{dz} \right)_a = G^2 \frac{d}{dz} \left( \frac{x^2 v_g}{\alpha} + \frac{(1-x)^2 v_f}{(1-\alpha)} \right) \quad (16)$$

Where  $\alpha$  is the void fraction, G is the mass flux, x is the mass quality, and  $\tilde{O}$  is the specific volume

## iii. The Homogeneous Model

The homogeneous model was used, considering the two phase flow can be treated as a single homogeneous phase possessing mean fluid properties [16]. For a steady homogenous flow, the basic equations reduce to the following form;

$$-\left(\frac{dP}{dz}\right) = 2 \frac{f_{TP}}{d} \bar{\rho} V_2^2 + \bar{\rho} g \tag{17}$$

Where “ $f_{TP}$ ” is the Fanning friction factor for the assumed homogeneous flow model, considering the two phases to flow as a single phase [14].  $\bar{\rho}$  is the homogenous fluid density [6] which is given by;

$$\bar{\rho} = \alpha \rho_g + (1 - \alpha) \rho_f \tag{18}$$

Thus, the pressure difference relationship is to be derived;

$$P_2 - P_0 = 2f_{TP} \frac{L}{d} \bar{\rho} V_2^2 + \frac{W}{A} \tag{19}$$

Where W is the weight of fluid in the bubble pump lift tube. Equation (19) is to be simplified by assuming that the density of the vapor phase is negligible compared to that of the liquid. Using the two phase relationships and Eq. (2), the pressure difference becomes;

$$P_2 - P_0 = 2f_{TP} \frac{L}{d} \bar{\rho} V_1^2 \left[ 1 + \frac{\dot{V}_g}{\dot{V}_f} \right]^2 + \frac{\rho_f g L}{1 + \left( \frac{\dot{V}_g}{\dot{V}_f} \frac{1}{s} \right)} \tag{20}$$

Where (s) is the slip ratio. Now, equating Eq. (20) with Eq. (4), one may find the ratio of the static head in the lower reservoir to the height of the lift tube as;

$$\frac{h}{L} = \frac{V_1^2}{2gL} \left[ 1 + \frac{2\dot{V}_g}{\dot{V}_f} + 4f_{TP} \frac{L}{d} \left( 1 + \frac{\dot{V}_g}{\dot{V}_f} \right)^2 \right] + \frac{1}{1 + \left( \frac{\dot{V}_g}{\dot{V}_f} \frac{1}{s} \right)} \tag{21}$$

Taking the friction factor for laminar liquid flow in a circular tube as  $f=64/Re$ , the above equation becomes;

$$\frac{h}{L} = \frac{128\mu_f}{\rho_f g d^2} V_2 + \frac{V_2^2}{2gL \left( \left( 1 + \frac{\dot{V}_g}{\dot{V}_f} \right)^2 \right)} + \frac{\dot{V}_g}{gL A \left[ 1 + \frac{\dot{V}_g}{\dot{V}_f} \right]} V_2 + \frac{1}{\left[ 1 + \frac{\dot{V}_g}{\dot{V}_f s} \right]} \tag{22}$$

According to the common practice in this field, the working fluid is selected to be Methyl Alcohol, CH<sub>3</sub>OH, or Methanol. Considering the number of the element control volumes is n along the pump lift tube indicated in Figure (4), the static pressure at the outlet from the n<sup>th</sup> element control volume can be calculated from the following equation;

$$P_n = P_0 + \frac{128L\mu_f V_{n-1}}{d^2} \left[ 1 + \frac{\dot{V}_g}{\dot{V}_f} \right] + \frac{\rho_f g L}{\left[ 1 + \frac{\dot{V}_g}{\dot{V}_f s} \right]} \tag{23}$$

While the heating power required to produce the desired vapor flow rate is,

$$\dot{Q} = \rho_g \dot{V}_g h_{fg} \tag{24}$$

Where  $h_{fg}$  is the latent heat of the working fluid at the working saturated temperature. Once the volumetric liquid flow rate is calculated, the mass flow rate of the pumped liquid may be calculated from the following known equation;

$$\dot{m}_f = \dot{V}_f \rho_f \quad (25)$$

More detailed derivation can be found elsewhere; Elshawesh [14].

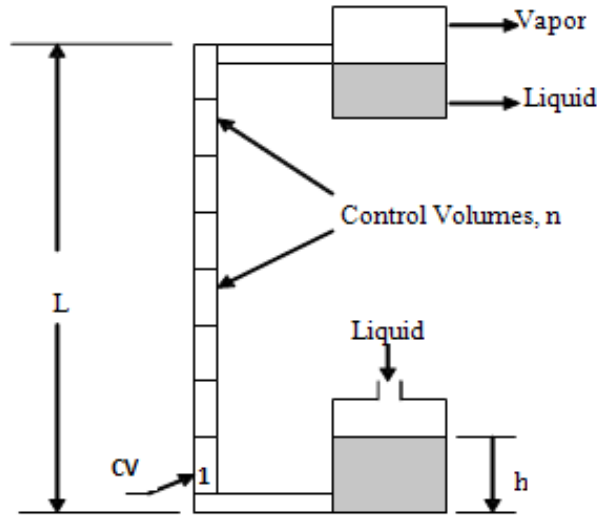


Figure (4). The lift tube is divided into small control volumes.

### 3. RESULTS AND DISCUSSIONS

The performance of the bubble pump is evaluated under different geometrical and operational conditions. Three different tube diameters are used;  $d=6, 8,$  and  $10\text{mm}$ . Three different driving heads are considered;  $h=0.45, 0.5,$  and  $0.55\text{m}$ , while the input heat is variable and it goes to  $500\text{W}$ . The present results are compared with published results presented in two recent experimental studies made by Sathe [5], master of the technology project report, and Koyfman, et al [7], a research paper. This comparison was made with the objective of validating and benchmarking the results of the present mathematical model. The following subsections present the effect of each of these design parameters on the pump performance.

#### i. Effect of the Driving Head

In this analytical study the driving heads were changed at three different levels and each level was studied individually to find out its effect on the mass flow rate of the pumped liquid with the increase of the heat input. For a tube diameter of  $10\text{mm}$ , Figure 5 shows that at low values of heat input, the mass flow rate drops slightly. This could be attributed to the high liquid viscosity resulting in high frictional force which in turn limits the buoyancy effects. However, as the input heat is increased, the viscosity decreases, the frictional force also decreases, resulting in an increase of both the buoyancy effect and the liquid mass flow rate of pumped liquid. This is clearly shown in Figure 5.

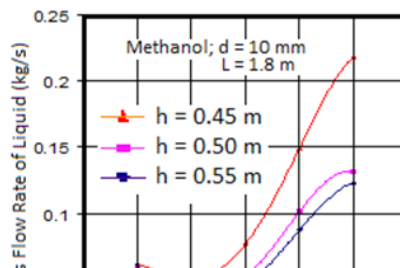


Figure (5). The variation of mass flow rate of pumped Methanol liquid for  $d = 10 \text{ mm}$  and  $L = 1.8 \text{ m}$ .

From Figure 5, it can be clearly seen that increasing the driving head decreases the mass flow rate for the same quantity of heat input. This result can be attributed to the fact that increasing the driving head means higher mechanical energy resistance and, therefore, lowering the mass flow rate. Increasing the driving head leads to a greater amount of liquid (in the lift tube) to be heated and, therefore, lowering the liquid temperature for the same amount of heat input resulting in a less chance of experiencing a two phase flow phenomena. It can also be noticed that, for each driving head, increasing the heat input results in a slight decrease in mass flow rate at the beginning and then after reaching a minimum value, the mass flow rate increases in almost a linear manner. This trend of the results has a fair agreement with the trend obtained by Koyfman et al [7], Figure 6.

On the other hand, lowering the driving head, within the range of the studied heads, the velocity of entering liquid to the bottom of the lift tube decreases, the flow resistance may increase and the temperature of the input heat rises resulting in a relatively higher vaporization rate and thus more vapor will be available to drive the liquid to the upper reservoir.

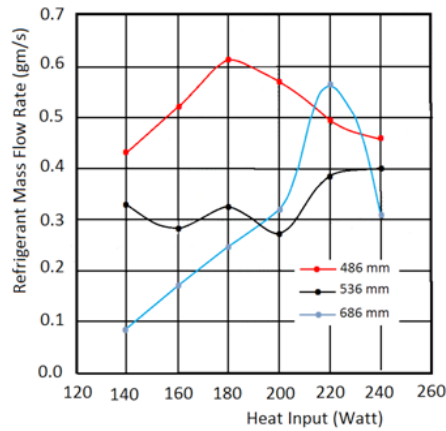


Figure (6). Variation of mass flow rate of pumped liquid for  $d = 10 \text{ mm}$  and  $L = 1.6 \text{ m}$ ; Koyfman, et al [7].

Figure (7) presents the effect of the static head obtained by Sathe [5]. Referring to the above results, it can be noticed that there is a difference among Sathe [5], the present study and the published Koyfman [7] results, where she found that the flow rate of the pumped liquid increases as the driving head is increased. However, the logical judgment goes with Koyfman et al and present trends.

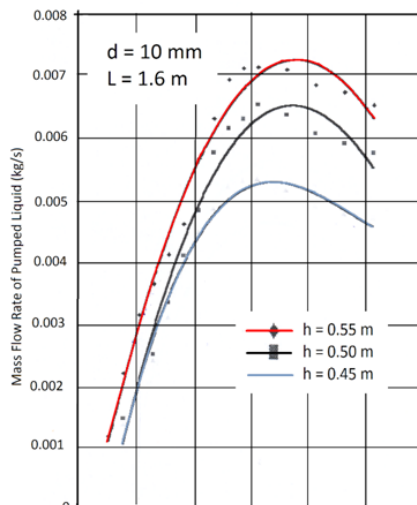


Figure (7). The variation of mass flow rate of pumped liquid for  $d = 10$  mm and  $L = 1.6$  m; Sathe [5].

*ii. Effect of the Pump Tube Diameter*

Figures (8 and 9) represent the relationship between the liquid mass flow rate and input heat for different tube diameters while the driving head is kept fixed at 0.45 and 0.55 m, respectively.

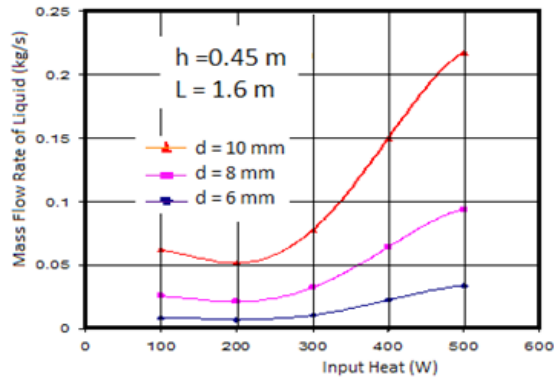


Figure (8). The variation of mass flow rate of pumped liquid with heat input for different tube diameters,  $h = 0.45$  m.

It was noticed that as the pump tube diameter increases the mass flow rate of the pumped liquid also increases with the increase of input heat. This may be justified, as the pump tube diameter increases, the frictional pressure drop decreases thereby decreasing the resistance to the flow motion. That is increasing the efficiency of the bubble pump and it results in increasing the liquid mass flow rate.

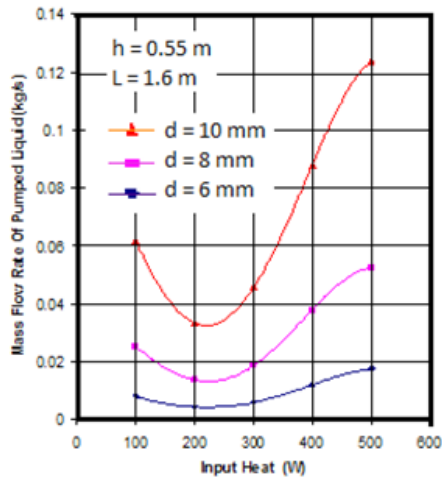


Figure (9) The variation of mass flow rate of pumped liquid for  $h = 0.55$  m and  $L = 1.6$  m; the present study.

The behavior of the bubble pump remains with the same trend for different tube diameters, that the mass flow rate of the pumped liquid decreases with heat input, reaches the minimum value and then will start increasing with further increase in the heat input. At high heat inputs of 500 W, the difference between

the liquid mass flow rates for 10 mm pump tube and 8 mm pump tube is much higher, about 200 %, than the difference between the liquid mass flow rates for 8 mm and 6 mm pump tubes. This is due to the high liquid flow rate gradient at high heat inputs. Around the heat input of 300 W, the obtained present results are similar to the results published by Sathe [5], Figure (10). This cannot be compared with the results obtained by Koyfman, et al [7], as they used one tube diameter only.

**iii. Variation of the Vapor Mass Flow Rate**

The vapor mass flow rate is directly proportional to the heat input. It is clear from Figure (11) that the driving head does not influence the vapor flow rate much. A lower driving head results in a slightly higher vapor flow rate. This is because of the decreased force exerted by the liquid column. The vapor flow rates are closely parallel along a range from the small values of the input heat to 300W and then the flow rate for driving head of 0.45 m slightly deviates from the other two curves.

This can be explained in that the vapor flow rate increases with the decrease in the driving head (h) at the high heat input. This means that as the flow rate decreases at the beginning of the thermal heating, the liquid temperature increases and consequently the formation of vapor bubbles increases which leads to an increase in the flow rate of the liquid rushing upwards to the top reservoir.

In this analytical study it was noticed that the vapor mass flow rate increases with the increase in the input heat, i.e. there is a direct relationship between the vapor mass flow rate and the input heat. This result agrees totally with the result obtained by Sathe [5], as shown in Figure (12), while Koyfman, et al [7], have not studied this relationship.

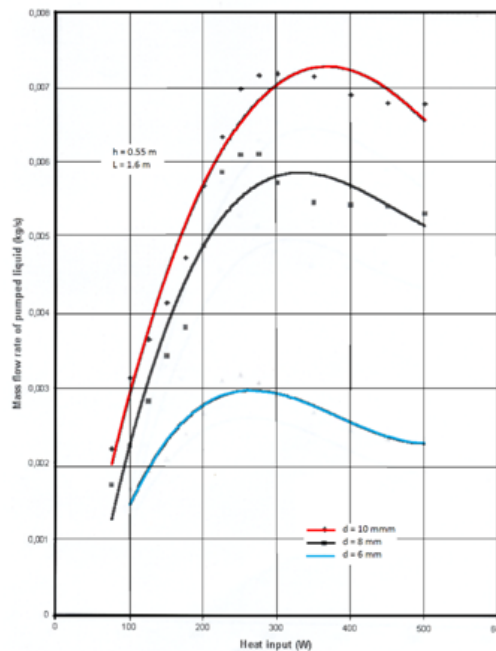


Figure (10). The variation of mass flow rate of pumped liquid for h = 0.55 m and L = 1.6 m; Sathe [5].

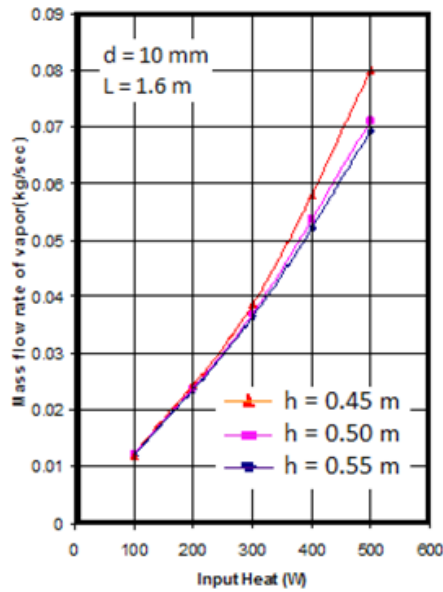


Figure (11). The variation of mass flow rate of vapor for  $d = 8 \text{ mm}$  and  $L = 1.6 \text{ m}$ ; the present study.

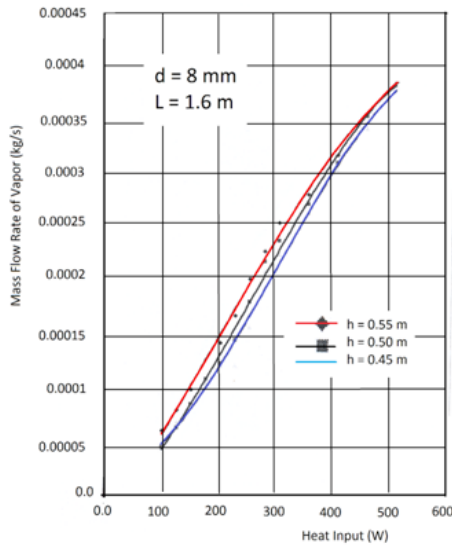


Figure (12). The variation of mass flow rate of vapor for  $d = 10 \text{ mm}$  and  $L = 1.6 \text{ m}$ ; Sathe [5].

#### 4. CONCLUSIONS

- A mathematical model is developed for the simulation of the behavior of the bubble pump, considering

the effects of the pipe diameter, driving static head, and heat input.

- The liquid and vapor mass flow rates are calculated for different geometrical and operating conditions.
- Through working with the driving head range, it was concluded that a low driving head is recommended to achieve a higher mass flow rate of the pumped liquid.
- Through working with the tube diameter range, it was concluded that increasing the thermal pump tube diameter results in an increase in mass flow rate of the pumped liquid.
- The obtained results have the same trend and in some cases they coincide with the other published results.

## 5. REFERENCES

- [1]. K.R. Ullah, R. Saidur, H.W. Ping, R.K. Akikur, N.H. Shuvo, *A review of solar thermal refrigeration and cooling methods Renewable and Sustainable Energy Reviews* 24 (2013) 499–513
- [2]. J. Aman, Paul F Henshaw, and David S-K Ting, *Modelling and Analysis of Bubble Pump Parameters for Vapor Absorption Refrigeration Systems*, 2016 ASHRAE Annual Conference June 25 - 29, 2016 St. Louis, MO USA.
- [3]. Delano Andrew, *Design Analysis of the Einstein Refrigeration Cycle*. Ph.D. Thesis, Georgia Institute of Technology, 1998.
- [4]. Xu, J.L., Huang X.Y., Wong, T.N., *Study on heat driven pump, Part 1- experimental measurements*, School of mechanical and production engineering, Nanyang Technological University, Nanyang Avenue, Singapore, *Int. Journal of Heat and Mass Transfer in press*, doi: 10.1016/S0017-9310(03)00144-3, 2003.
- [5]. Sathe, A., *Experimental and theoretical studies on a bubble pump for a diffusion absorption refrigeration system*, Master of Technology Project Report, Universitat Stuttgart, 2001.
- [6]. Jennifer White, S., *Bubble pump design and performance*, Master of Science in Mechanical Engineering, Georgia Institute Of Technology, 2001.
- [7]. Koyfman A., M. Jelinek, A. Levy, I. Borde, *An experimental of bubble pump performance for diffusion absorption refrigeration system with organic working fluids*, Mechanical Engineering Department, Ben-Gurion University of the Negev, Israel, *Applied Thermal Engineering*, doi: 10.1016/S1359-4311(03)00162-5, 2003.
- [8]. A. Benhmidene, B. Chaouachi and S. Gabsi, *A Review of Bubble Pump Technologies*. *Journal of Applied Sciences*, 10, 2010, 1806-1813.
- [9]. Chung Han-Shik, Woo Ju-Sik, Shin Yong-Han, Kim Jun-Hyo, Jeong Hyo-Min, *Experimental Assessment Of Two-Phase Bubble Pump For Solar Water Heating*, *J. Cent. South Univ.* (2012) 19: 1590-1599
- [10]. Zohar, A., M. Jelinek, A. Levy and I. Borde, 2008. *The influence of the generator and bubble pump configuration on the performance of Diffusion Absorption Refrigeration (DAR) system*. *Int. J. Refrigeration*, 31: 962-969.
- [11]. Jakob, U., U. Eicker, A.H. Taki and M.J. Cook, 2005. *Development of a solar powered diffusion absorption cooling machine*. *Proceedings of the 1st International Conference Solar Air-Conditioning*, Oct. 6-7, Staffelstein, Germany, pp: 111-115.
- [12]. Jakob, U., U. Eicker, D. Schneider, M.J. Cook and A.H. Taki, 2008. *Simulation and experimental investigation into diffusion absorption cooling machines for air-conditioning applications*. *Applied Ther. Eng.*, 28: 1138-1150.
- [13]. Benhmidene, A., K. Hidouri, B. Chaouachi, S. Gabsi, M. Bourouis and A. Coronas, 2008. *Two-fluid model for simulation of the diphasic flow in solar bubble pump*. *Proceedings of the International Sorption Heat Pump Conference*, September 23-26, Seoul, Korea.
- [14]. Elshawesh, K. O., *Heat Driven Bubble Pump*, M. Sc. Thesis, Mechanical Engineering Department, School of Engineering and Applied Sciences, Academy of Graduate Studies, Tripoli-Libya 2008.
- [15]. Merle C. Potter, David C. Wiggert, *Mechanics Of Fluids*. Second Edition, Prentice-Hall, Inc. Simon and Schuster/A Viacom Company Upper Saddle River, NJ, 1997.

[16]. Collier John, G., *Convective Boiling and Condensation*, Oxford Science Publications, Second Edition, 1980.

## **BIOGRAPHIES**

*The first author (Eng. Khaled Elshawesh) graduated in 2008 with an M.Sc. degree in Mechanical Engineering from the School of Engineering and Applied Sciences, Academy of Graduate Studies, Tripoli-Libya, and currently working as an a researcher in the field of thermal fluid sciences at the Central Board for Research and Manufacturing based in Tripoli-Libya. The second and third authors (Agha and Dekam) are professors at the Mechanical Engineering Department, University of Tripoli and their research interests are in the fields of fluid mechanics, heat transfer and thermal energy conversion.*

*Dr. Khairy had died and left an impressive history and achievements, and proper behaviour; knowledge and research. This paper shows a sample of the broad research activity especially related to solar applications that he loves so much, the mercy of Allah almighty.*